Supporting Information

Loosely stacked lamellar membrane by irregular MoS_2 flakes for ultrahigh water and organics permeation

Xulin Cui[a,1], Xiaoli Wu[a,1], Jie Zhang[a], Jingtao Wang[a,*], Haoqin Zhang[a], Fengguang Du[b], Lingbo Qu[b], Xingzhong Cao[c], Peng Zhang[c]

[a]School of Chemical Engineering and Energy, Zhengzhou University, Zhengzhou 450001, P. R. China

[b]State Key Laboratory of Motor Vehicle Biofuel Technology, Nanyang 473000, P.R. China

[c]Multi-discipline Research Division, Institute of High Energy Physics, Chinese Academy of Sciences, Beijing 100049, China

*To whom correspondence should be addressed: E-mail: jingtaowang@zzu.edu.cn (J.T. Wang).

[1]These authors contributed equally to this work.

Supplementary Figures

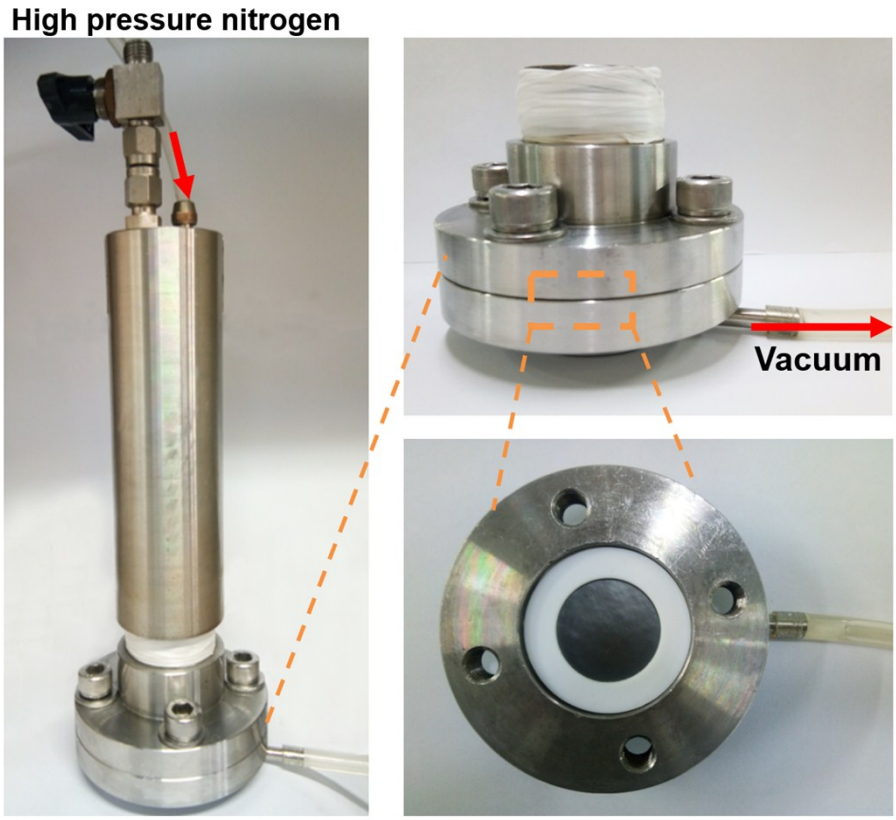

Fig. S1. The home-made experimental apparatus for the preparation and performance measurement of the membranes.

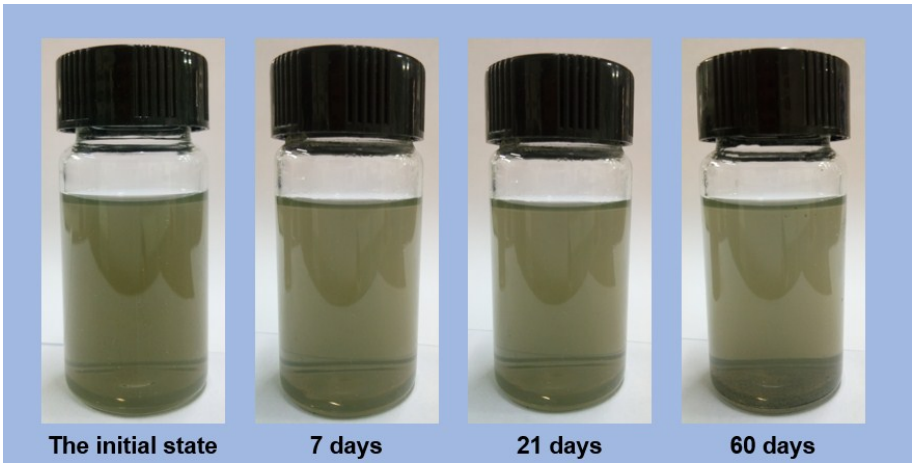

Fig. S2. Photographs of dispersion of MoS_2 flakes at different times.

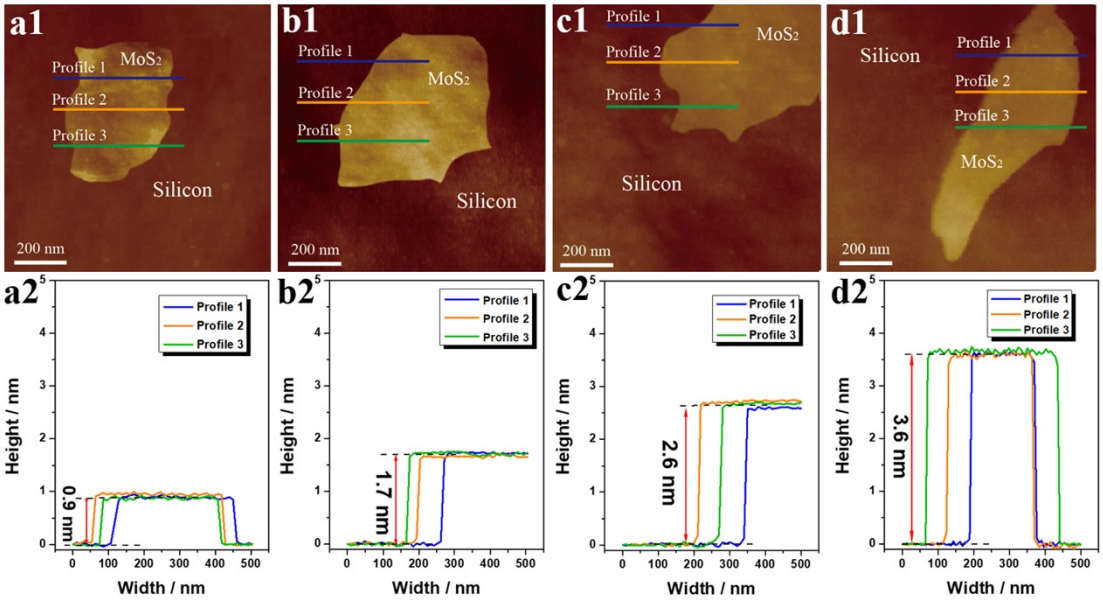

Fig. S3. AFM images and corresponding height profiles of MoS_2 flakes with thickness of (a) 0.9 nm, (b) 1.7 nm, (c) 2.6 nm, and (d) 3.6 nm.

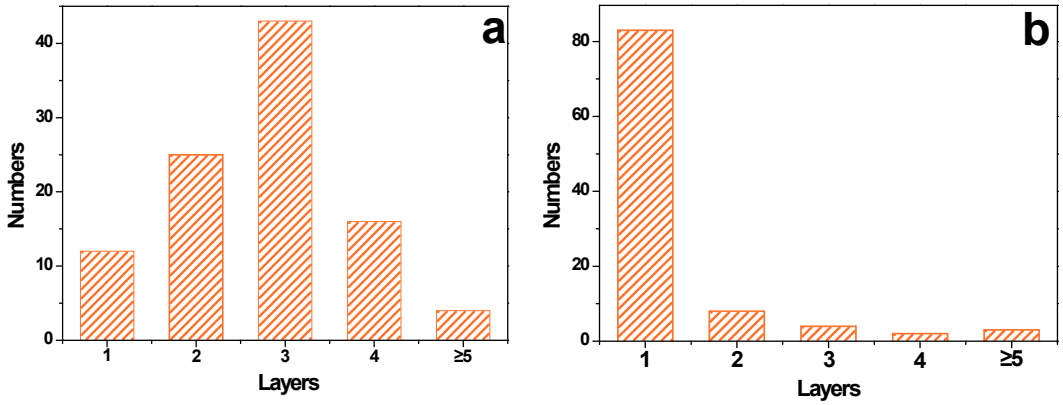

Fig. S4. Layer distribution of MoS_2 flakes in the AFM diagrams, dispersion solution a (a) and dispersion solution b (b).

The MoS_2 dispersion was fabricated through a temperate ultrasonic-assisted exfoliation method and centrifuged at (a) 3000 rpm and (b) 7000 rpm for 10 min, respectively, to obtain the dispersion solution a and b. Then the solutions were transferred to monocrystalline silicon for AFM testing, and the thickness curves were measured to analyze and count the numbers of layers.

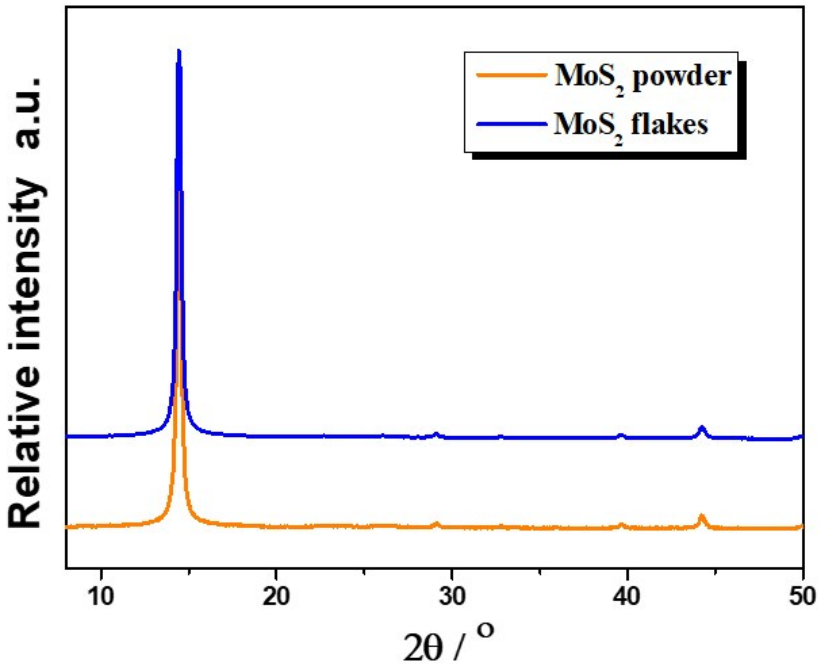

Fig. S5. XRD curves of MoS_2 powder and flakes.

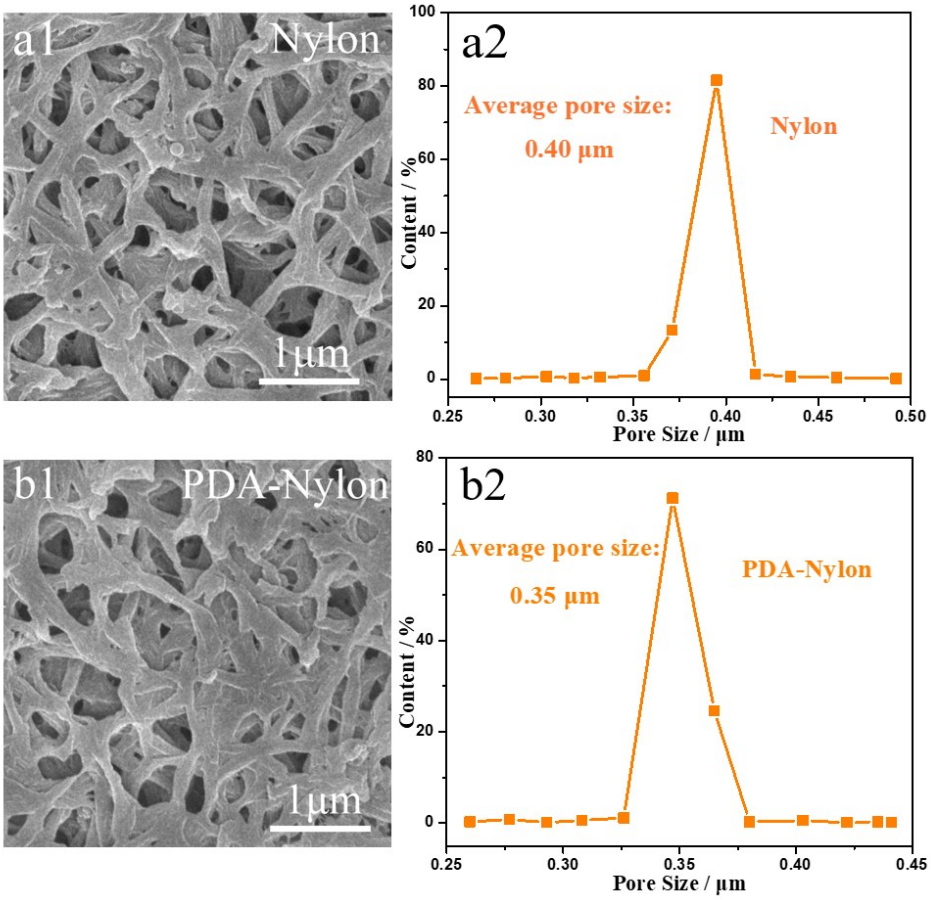

Fig. S6. SEM images and the distribution of pore size for (a) Nylon and (b) PDA-Nylon support.

MoS_2 membrane thickness measurement

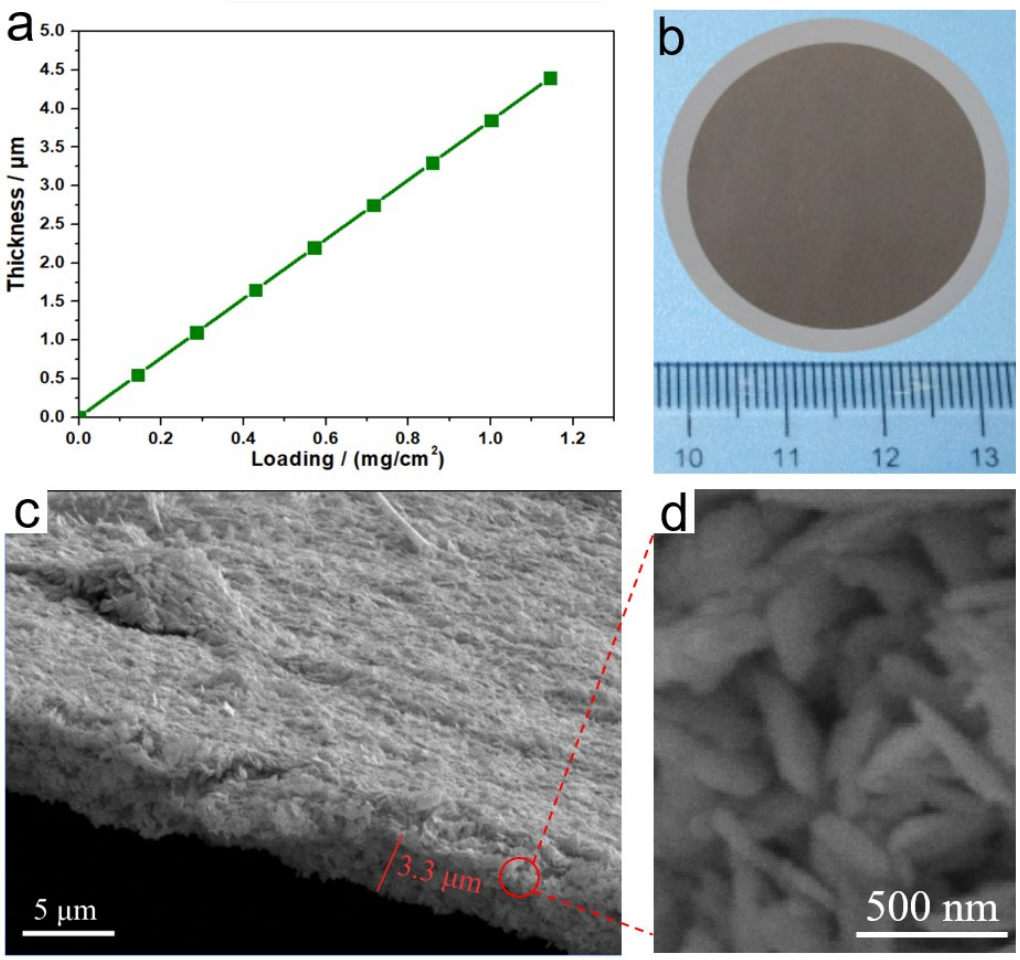

Fig. S7. (a) Variation of the membrane thickness as a function of flakes loading. (b) A photo of as-prepared MoS_2 membrane. (c and d) Cross-sectional SEM images of MoS_2 membrane.

The linear relationship between MoS_2 loading and membrane thickness was determined by cross-sectional SEM. Specifically, the MoS_2 dispersion was filtrated under vacuum through the PDA-modified nylon support with 0.35 μm pore size to obtain the MoS_2 membranes. The thicknesses of prepared membranes are 0.6, 1.2, 1.7, 2.3, 2.9, 3.5, 4.0 and 4.6 μm, respectively.

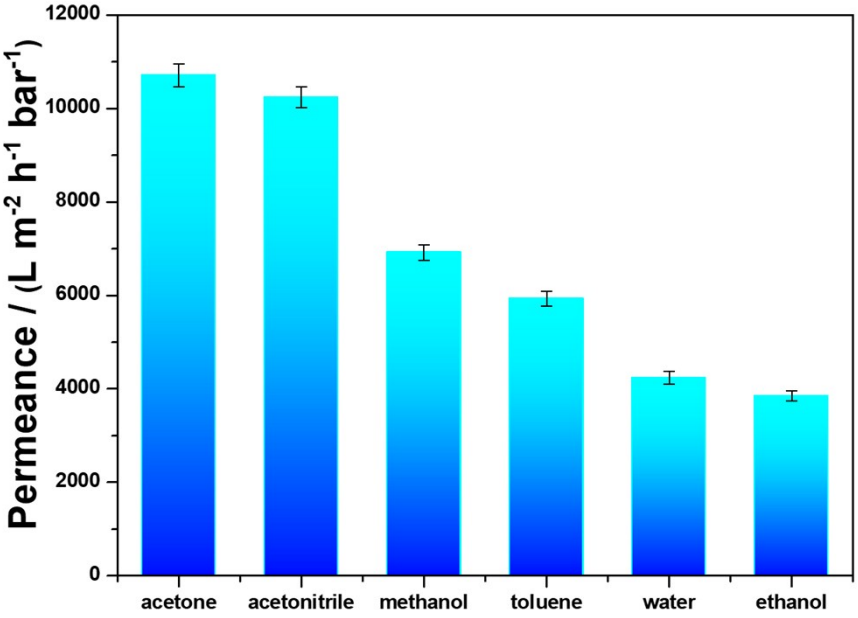

Fig. S8. Solvent permeance of Nylon support.

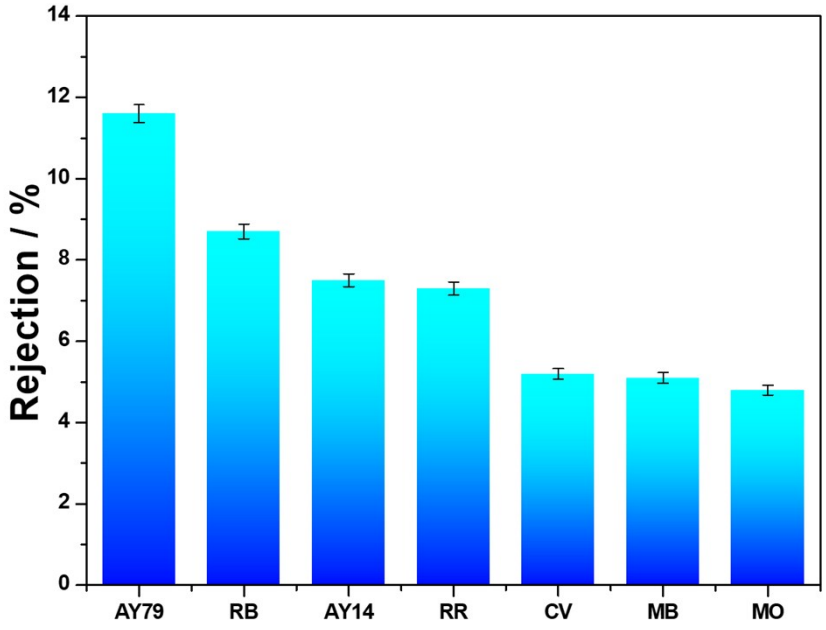

Fig. S9. Rejection of different dye molecules of Nylon support.

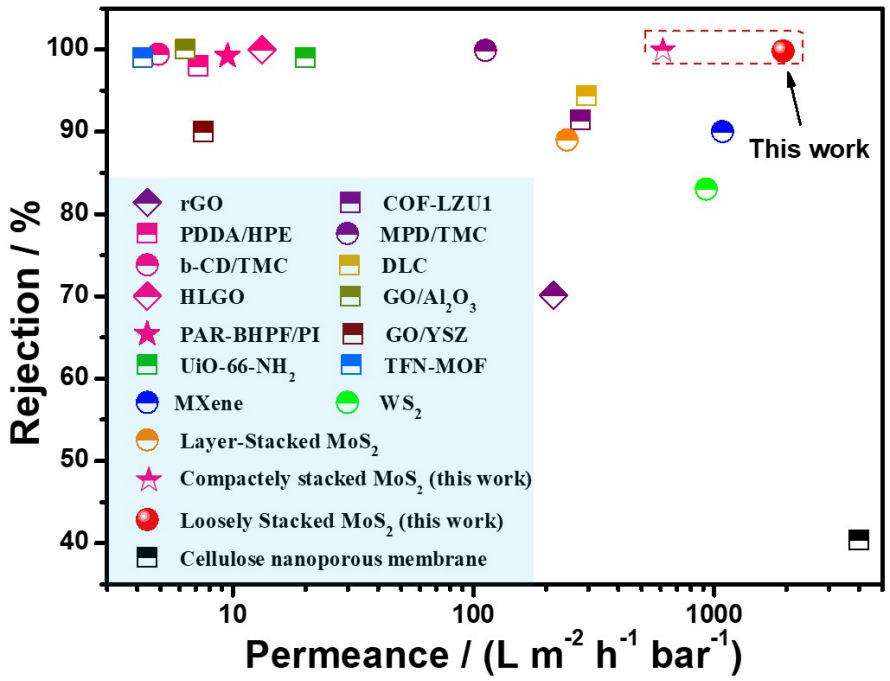

Fig. S10. Performance comparison between MoS_2 membrane in this study and various previously reported membranes.

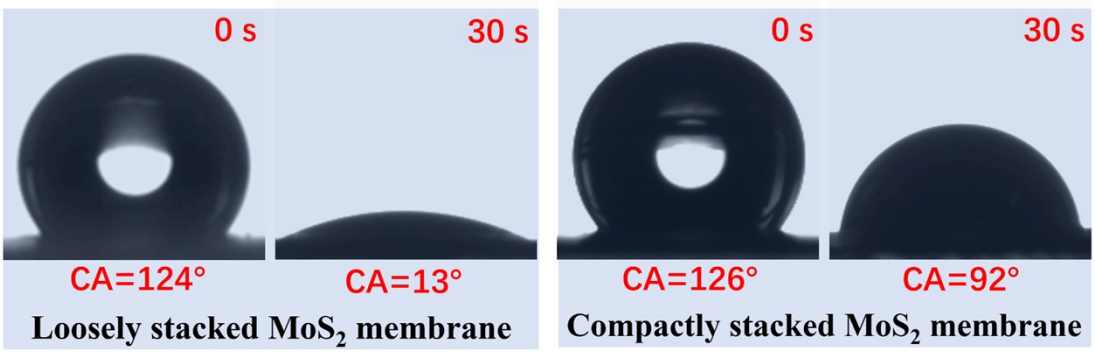

Fig. S11. Water contact angles of loosely attacked MoS_2 membrane and compactly stacked MoS_2 membrane.

The loosely stacked membrane and compactly stacked membrane show similar water contact angle (124^o vs 126^o) in the initial state due to the hydrophobic nature. However, the water contact angle of loosely stacked MoS_2 membrane dramatically reduced to 13^o within 30 s, while it relatedly reduced to 92^o for compactly stacked membrane. The similar contact angles in the initial state indicate that the layer number might have a negligible influence on the hydrophilic/hydrophobic nature of membrane. Meanwhile, the difference in the reduction degree of contact angle within 30 s implies that loosely stacked membrane has a stronger ability to dissolve molecules than compactly stacked membrane. This phenomenon may be attributed to the rough surface structure of loosely stacked membrane, which gives solvent molecules the ability to rapidly enter interlayer channels.

.

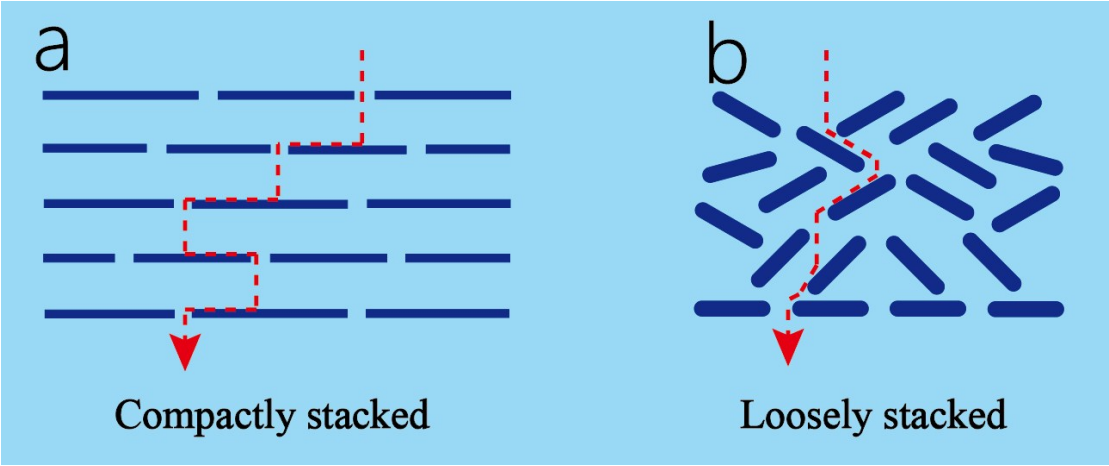

Fig. S12. Comparison of fluid molecular transport paths between (a)compactly stacked and (b) loosely stacked MoS_2 membranes.

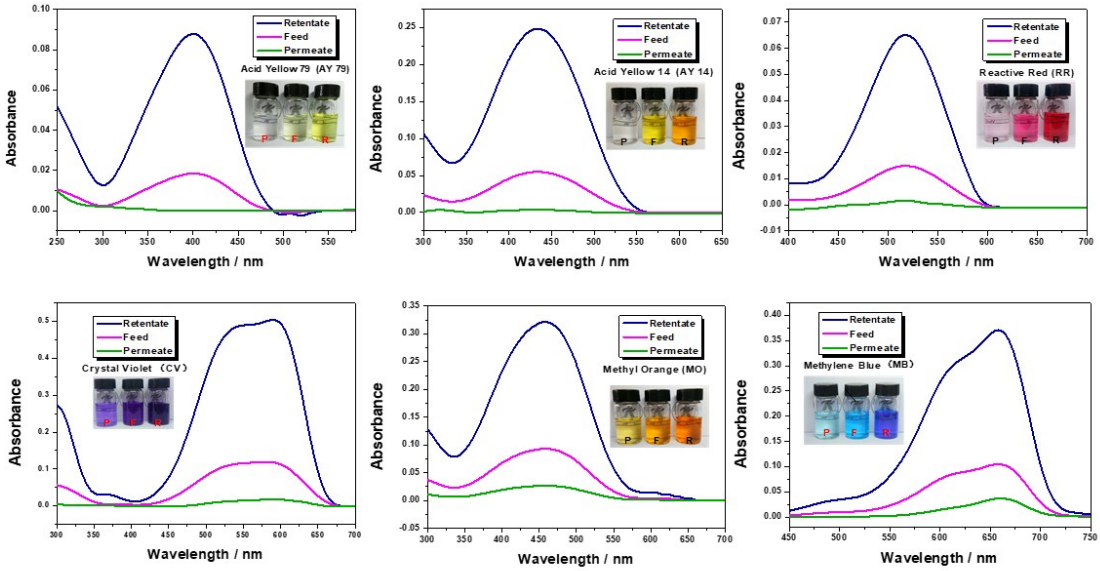

Fig. S13. UV-vis absorption spectra of a series of dye molecules in methanol before and after filtration through the MoS_2 membrane (inserts are retentate, feed and permeate solution).

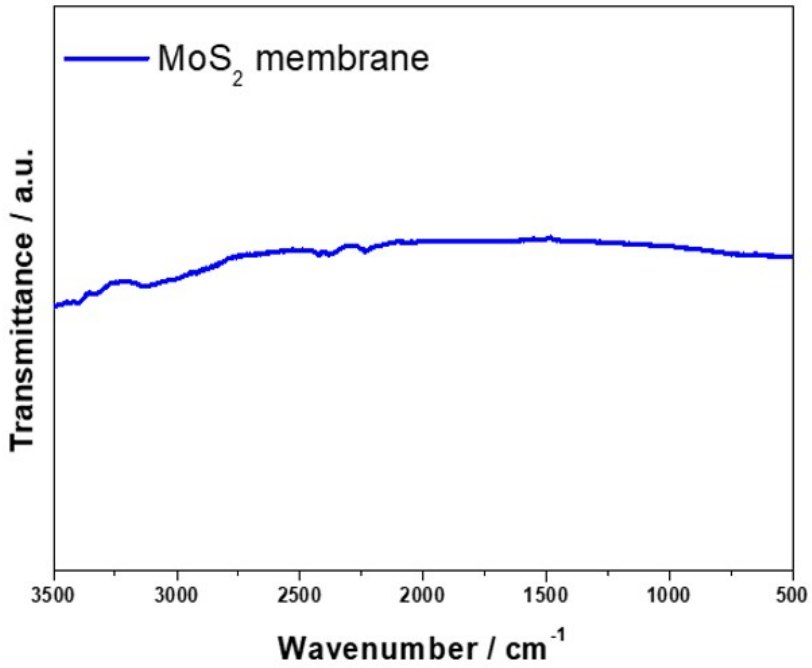

Fig. S14. FTIR curve of MoS_2 membrane.

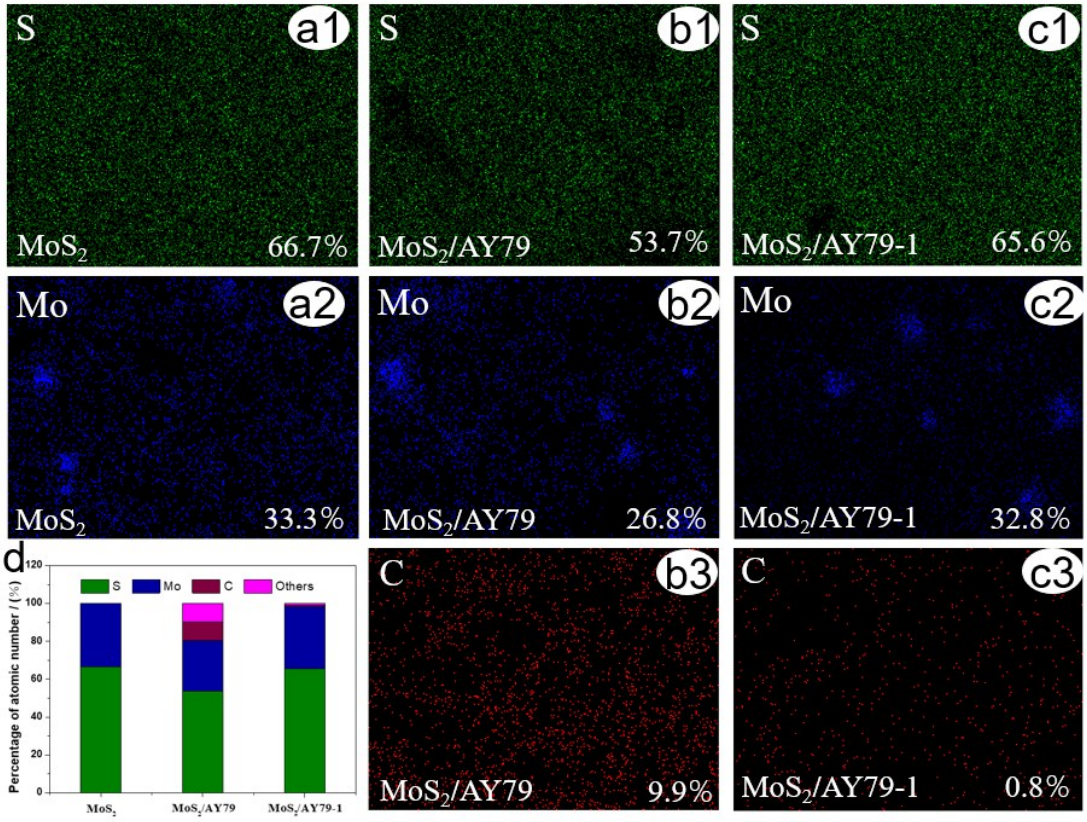

Fig. S15. EDS images of (a) MoS_2 membrane before rejection measurement, (b) the front and (c) back of membrane after rejection of AY79. (d) Percentage of atomic number of MoS_2 membrane in different states.

It is noteworthy that after AY79 molecules were separated through MoS_2 membrane, abundant C element appeared on the front of membrane, while almost no C element was detected on the back side of membrane. This phenomenon indicates that the dye molecules are excellently rejected by this membrane.

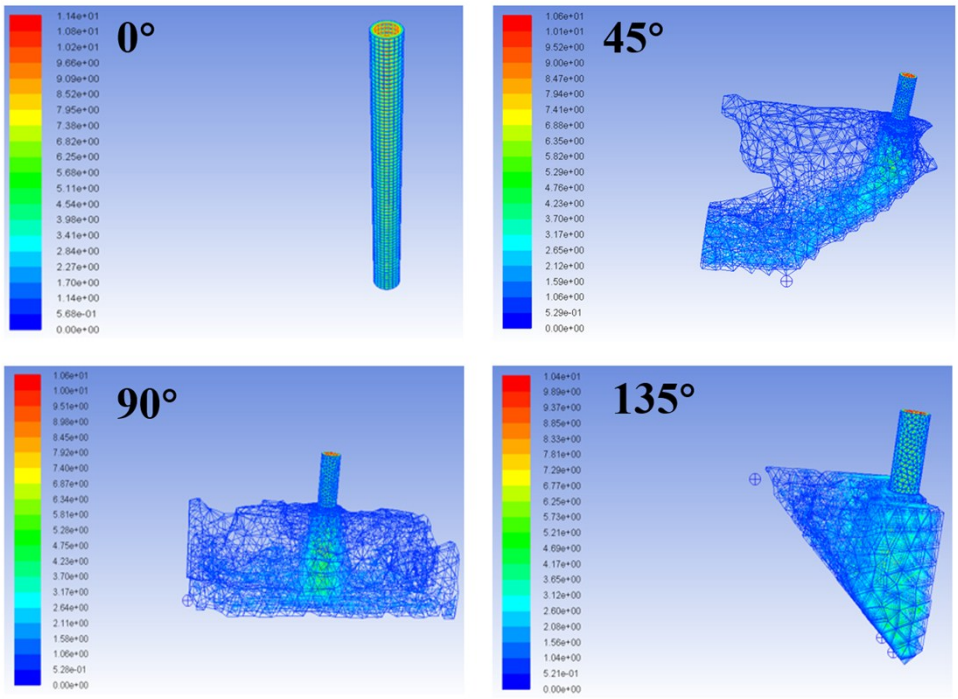

Fig. S16. Velocity cloud diagrams of fluid flowing over flakes at different tilt angles.

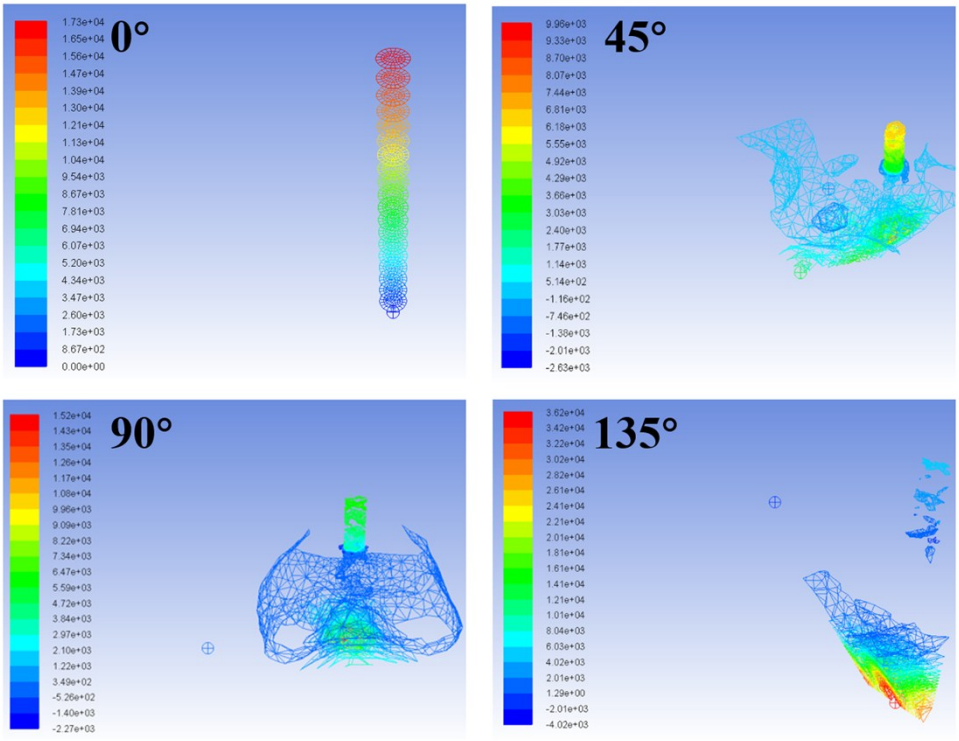

Fig. S17. Pressure cloud diagrams of fluid flowing over flakes at different tilt angles.

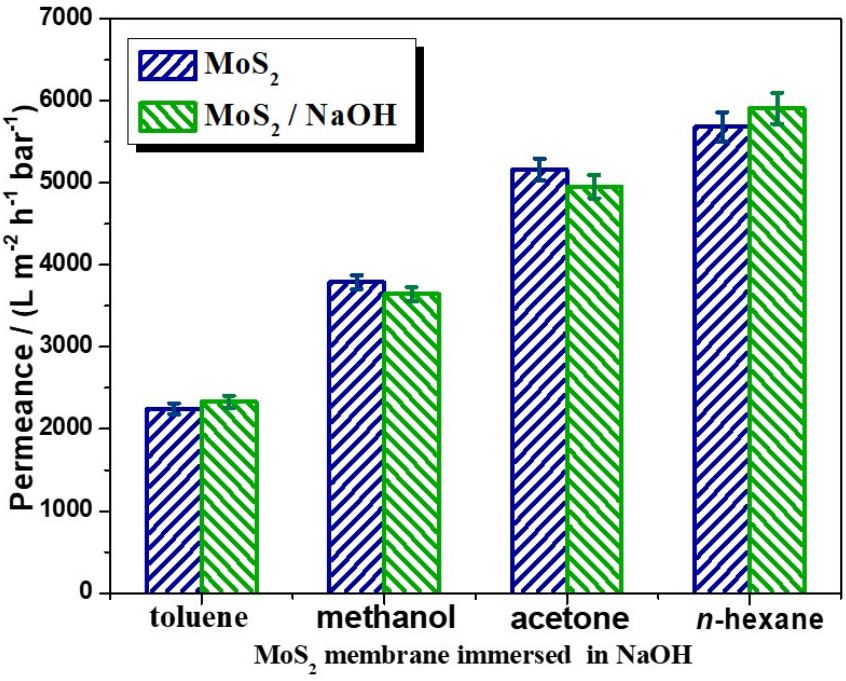

Fig. S18. Permeance variations of toluene, methanol, acetone and *n*-hexane of MoS_2 membrane after immersing in NaOH solution (pH = 10) for 24 h.

Supplementary Tables

Table S1. Calculation of positron penetration depth.

Number	Quality (g)	Volume (cm^3)	Density ($g\ cm^{-3}$)	Penetration depth (nm)
1	0.00455	1.61×10^{-3}	2.83	1706
2	0.00462	1.61×10^{-3}	2.87	1682
3	0.00457	1.61×10^{-3}	2.81	1718
average value	0.00458	1.61×10^{-3}	2.84	1700

The quality of the MoS_2 is obtained by subtracting Nylon from dry membrane. The volume is calculated by multiplying the effective membrane area (7 cm^2) by the thickness (2.3 μm) of the membrane. The positron penetration depth (R, nm) is calculated by the formula[9]:

$$R = (40 / \rho) \times E^{1.6}$$

Where ρ is the density ($g\ cm^{-3}$) and E is the positron energy (keV). To ensure the accuracy of the measurement, the same test was repeated three times and the average value was taken.

Table S2. Comparison of the separation performance for various membranes.

Membrane	Thickness (μm)	Solute	Size (nm)	Water permeance ($L\ m^{-2}\ h^{-1}\ bar^{-1}$)	Rejection (%)	Reference
MoS_2	2.3	AY79	2.3×2.8	1432	99.8	This Work
MoS_2	1.65	AY79	2.3×2.8	1625	99.8	This Work
Compactly-stacked MoS_2	1.5	AY79	2.3×2.8	538	99.9	This Work
Layer-stacked MoS_2	1.8	Evans Blue	3.4×1.3	245	89	1
Nanostrands-channeled GO	2	Evans Blue	3.4×1.3	695	84	2
GO	2	Evans Blue	3.4×1.3	71	85	3
MXene	0.4	Evans Blue	3.4×1.3	1084	90	4
MXene	0.4	Cytochrome c	2.5×3.7	1056	97	4
COF	290	Methylene Blue	0.7×1.5	125	98	5
WS_2	0.5	Evans Blue	3.4×1.3	450	89	6
SWCNT-intercalated GO	0.04	Cytochrome c	2.5×3.7	700	98.3	7
rGO	0.018	Brilliant Yellow	2.6×1.2	88.3	99.2	8

Table S3. Molecular properties of different dyes and rejection after filtration through MoS_2 membrane.

Dye molecular	MW (g / mol)	Size (nm)	Charge	Methanol permeance (L m^{-2} h^{-1} bar^{-1})	Rejection (%)
MB	373.9	1.2	+	3710 ± 52	50.8 ± 2.3
MO	327.3	1.2	-	3588 ± 41	58.5 ± 2.1
CV	408.0	1.5	+	3682 ± 55	70.2 ± 1.6
RR	788.3	1.5	-	3532 ± 48	73.7 ± 1.5
AY14	449.2	1.9	-	3547 ± 46	91.7 ± 1.2
RB	991.8	2.0	-	3539 ± 47	94.6 ± 1.1
AY79	1111.1	2.8	-	3521 ± 45	99.8 ± 0.6

Table S4. The calculated adsorption of dye molecules in MoS_2 membrane.

Dye molecular	Feed concentration (mg L^{-1})	Permeate concentration (mg L^{-1})	Retentate concentration (mg L^{-1})	Dye absorption (%)
MB	10	3.52	34.51	2.79
MO	10	2.75	37.07	3.85
CV	10	1.43	42.52	3.54
RR	10	1.13	43.56	3.82
AY14	10	0.78	45.26	3.23
RB	10	0.49	46.09	3.92
AY79	10	0.02	48.04	3.77

The adsorption ratio of dye molecules through the 2.3-μm-thick MoS_2 membrane is calculated by concentration change. 0.2 L of 10 mg L^{-1} dye molecules are used as feed solution, and the amount of the permeate solution and retentate solution are controlled to be 160 ml, 40 ml, respectively. The mass of dye molecules in feed is 0.2 × F, *i.e.* 0.2 × 10 = 2. And the mass of dye molecules in permeate and retentate are 0.16 × P and 0.04 × R, respectively. According to mass conservation, the mass of absorbed dye molecules is 0.2 × F – 0.16 ×P – 0.04 × R. Therefore, the adsorption ratio of dye molecules is the adsorption mass / total mass × %, *i.e.* (0.2 × F – 0.16 ×P – 0.04 × R) / 2 × %.

Thereby, the adsorption ratio of dye molecules is calculated by the formula:[10,11]

$$Dye\ absorption\ (\%) = (0.2 \times F - 0.16 \times P - 0.04 \times R) / 2 \times \%$$

Where F is the feed concentration (mg L^{-1}), P is the permeate concentration (mg L^{-1}), and R is retentate concentration (mg L^{-1}), which are determined by UV–vis technique.

Table S5. Element distribution of AY79.

Atomic name	Atomic number	Quantity ratio (%)	Relative atomic mass	Atomic mass ratio (%)
C	47	40.9	12.01	50.8
H	40	34.8	1.01	3.6
N	10	8.7	14.01	12.6
Na	2	1.7	22.99	4.1
O	12	10.4	16.00	17.3
S	4	3.5	32.07	11.5

The molecular formula of AY79 is $C_{47}H_{40}N_{10}Na_2O_{12}S_4$, and the proportion of C element is clearly observed to be the highest one. Meanwhile, considering that there are only two elements of Mo and S in MoS_2, the C element is chosen as a unique marker element for AY79.

Supplementary References

1. L. Sun, H. Huang and X. Peng, *Chem. Commun.*, 2013, **49**, 10718−10720.
2. H. Huang, Z. Song, N. Wei, L. Shi, Y. Mao, Y. Ying, L. Sun, Z. Xu and X. Peng, *Nat. Commun.*, 2013, **4**, 2979.
3. H. Huang, Y. Mao, Y. Ying, Y. Liu, L. Sun and X. Peng, *Chem. Commun.*, 2013, **49**, 5963−5965.
4. L. Ding, Y. Wei, Y. Wang, H. Chen, J. Caro and H. Wang, *Angew. Chem. Int. Ed.*, 2017, **56**, 1825−1829.
5. S. Kandambeth, B. P. Biswal, H. D. Chaudhari, K. Rout, H. Kunjattu, S. Mitra, S. Karak, A. Das, R. Mukherjee, U. K. Kharul and R. Banerjee, *Adv. Mater.*, 2017, **29**, 1603945.
6. L. Sun, Y. Ying, H. Huang, Z. Song, Y. Mao, Z. Xu and X. Peng, *ACS Nano*, 2014, **8**, 6304−6311.
7. S. Gao, H. Qin, P. Liu and J. Jin, *J. Mater. Chem. A*, 2015, **3**, 6649−6654.
8. L. Huang, J. Chen, T. Gao, M. Zhang, Y. Li, L. Dai, L. Qu and G. Shi, *Adv. Mater.*, 2016, **28**, 8669−8674.
9. B. Li, W. Liu, Z. Jiang, X. Dong, B. Wang and Y. Zhong, *Langmuir*, 2009, **25**, 7368−7374.
10. X. Zheng, G. Shen, C. Wang, Y. Li, D. Dunphy, T. Hasan, C. J. Brinker and B.-L. Su, *Nat. Commun.*, 2017, **8**, 14921.
11. F. Q. Wang, M. Hu and Q. Wang, *J. Mater. Chem. A*, 2019, **7**, 6259−6266.